Supporting Information

Tetraphenylethene-capped aminobenzopyranoxanthene hydrazone probes for colorimetric recognition of Hg^{2+} and fluorescent sensing of HCl gas

Yang Yang[a,b*], Chang Pei[a], Chao-Ying Gao[a], and Jinglin Liu[a,b*]

[a]*College of Chemistry and Materials Science, Inner Mongolia Minzu University, Tongliao 028043, PR China;*

[b]*Inner Mongolia Key laboratory for the Natural Products Chemistry and Functional Molecular Synthesis, Tongliao 028043, PR China*

E-mail addresses: yangyang-000@163.com (Y.Yang); jlliu@126.com (J.Liu)

Content

1. Synthesis route of ABPX-TPE1 and ABPX-TPE2.

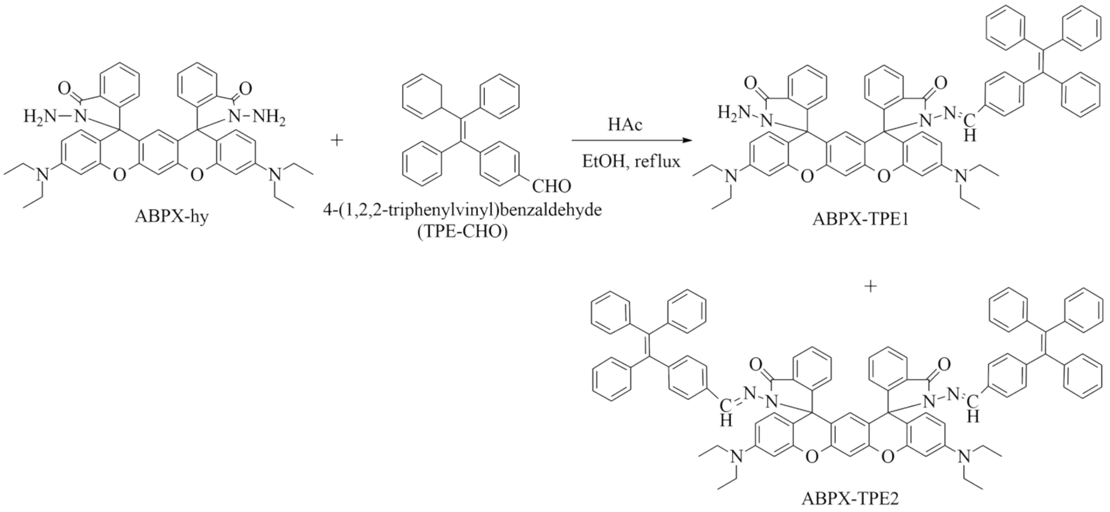

2. Theoretical calculations.

All calculations were performed by ORCA 5.0.1[S1]. All geometrical structures were optimized by density functional theory at PBE0-D3/def2-SVP level[S2]. Vibrational frequency analyses at the same level as optimization were performed to confirm that all stationary points were local minimum (no imaginary frequency). The ethanol was served as solvent, using the Conductor-like Continuum Polarization Model (C-PCM)[S3]. The high-level PBE0-D3/def2-TZVP and the Solvation Model based on Density (SMD) model[S4] were used to calculate the electronic energy on the basis of optimized structures.

The wave function-related topological studies were performed using Multiwfn software[S5] and visualization by VMD software[S6].

3. References.

[S1] a) F. Neese, Wiley Interdisciplinary Reviews: Computational Molecular Science 2018, 8, e1327; b) F. Neese, Wiley Interdisciplinary Reviews: Computational Molecular Science 2012, 2, 73-78.

[S2] a) F. Weigend, R. Ahlrichs, PCCP 2005, 7, 3297-3305; b) F. Weigend, PCCP 2006, 8, 1057-1065.; c) S. Grimme, J. Antony, S. Ehrlich, H. Krieg, J. Chem. Phys. 2010, 132, 154104; d) S. Grimme, S. Ehrlich, L. Goerigk, J. Comput. Chem. 2011, 32, 1456-1465; e) V. Barone, M. Cossi, J. Phys. Chem. A 1998, 102, 1995-2001.

[S3] Barone, V.; Cossi, M. (1998) J. Phys. Chem. A, 102, 1995.

[S4] Marenich, A. V.; Cramer, C. J.; Truhlar, D. G. (2009) J. Phys. Chem. B, 113, 6378.

[S5] T. Lu, F. Chen, J. Comput. Chem. 2012, 33, 580-592.

[S6] W. Humphrey, A. Dalke, K. Schulten, VMD: Visual Molecular Dynamics, J. Mol. Graphics 14 (1996) 33.

4. The characterization of ABPX-hy.

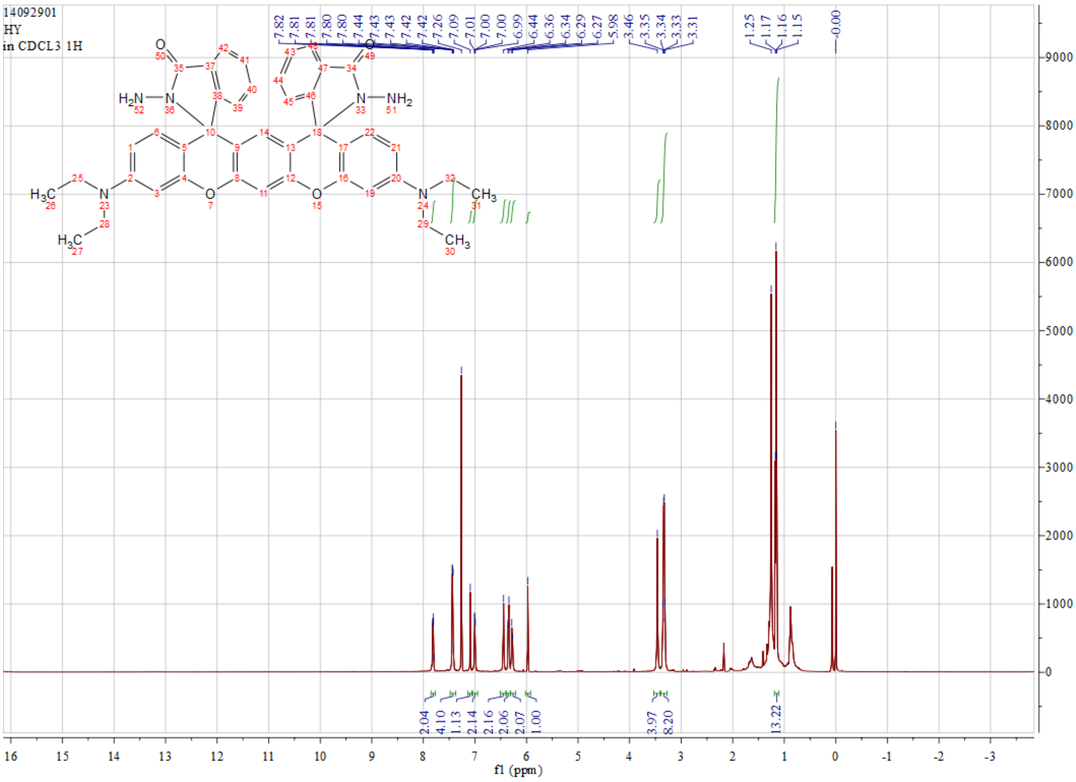

^{1}H NMR

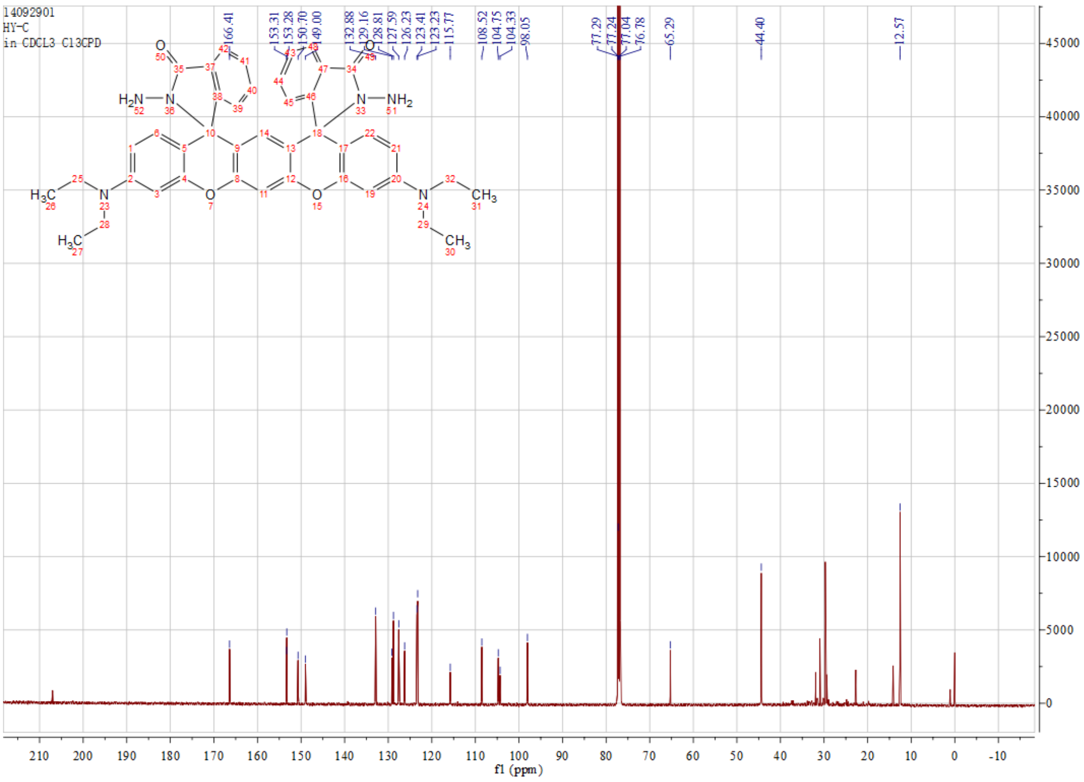

^{13}C NMR

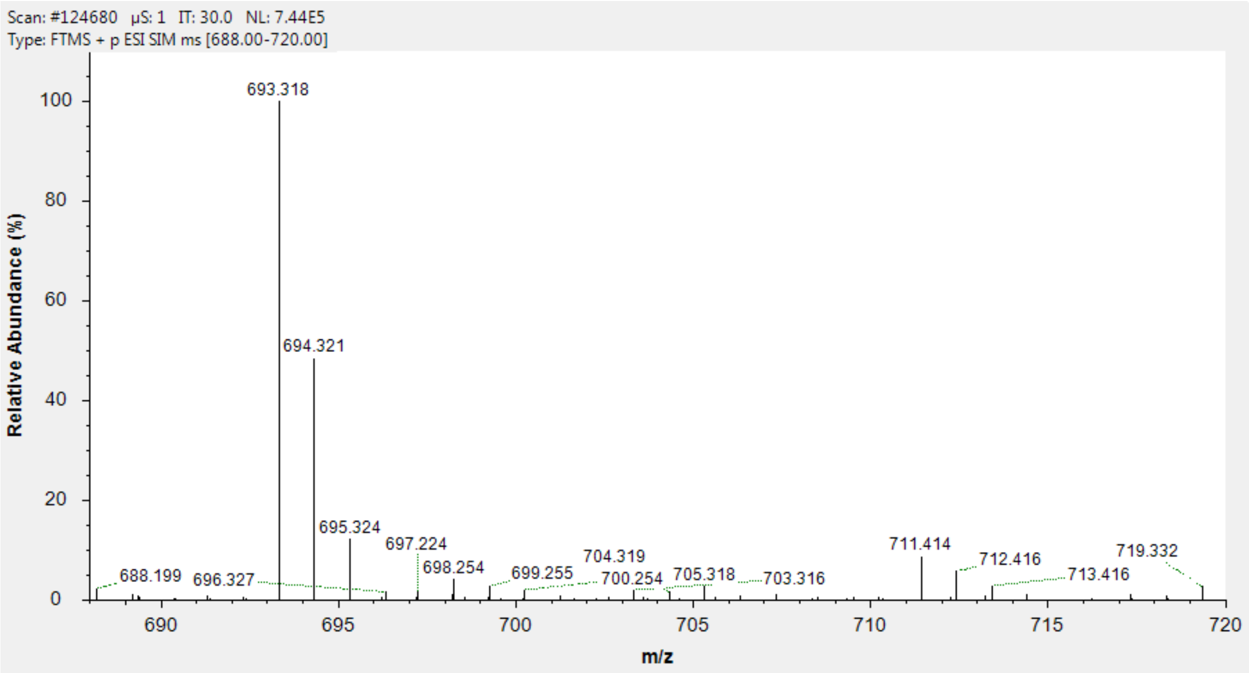

ESI-MS (M+H$^+$: m/z = 693.318)

5. The characterization of A-T1.

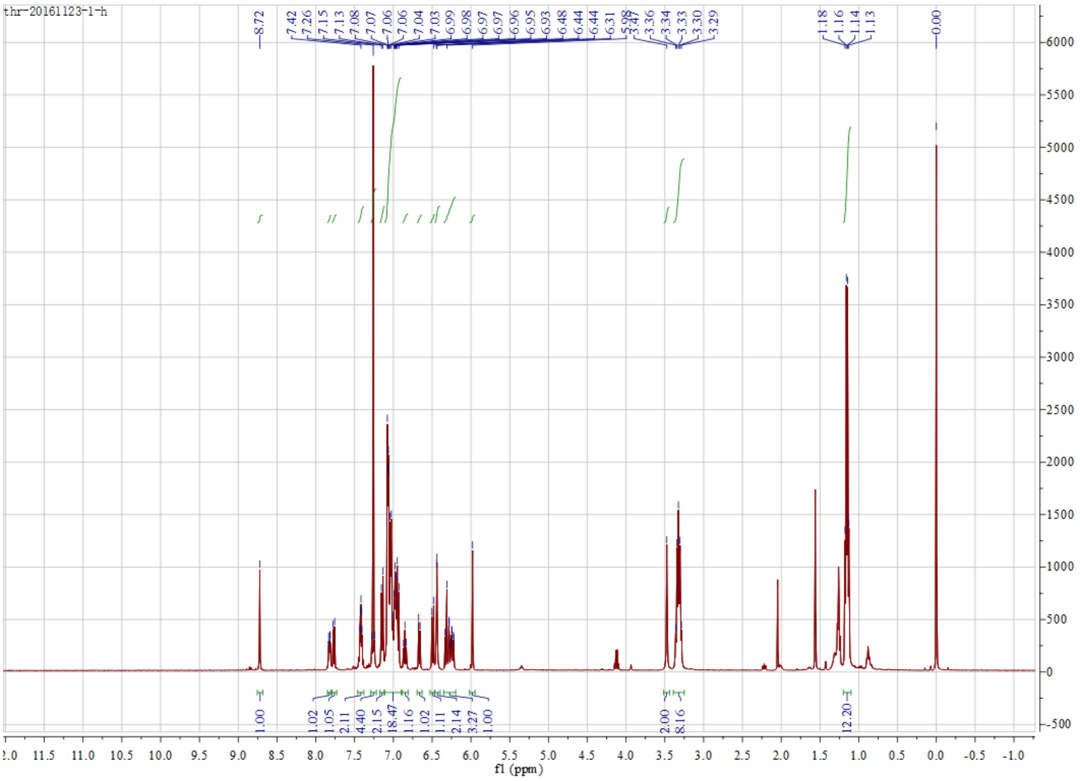

¹H NMR

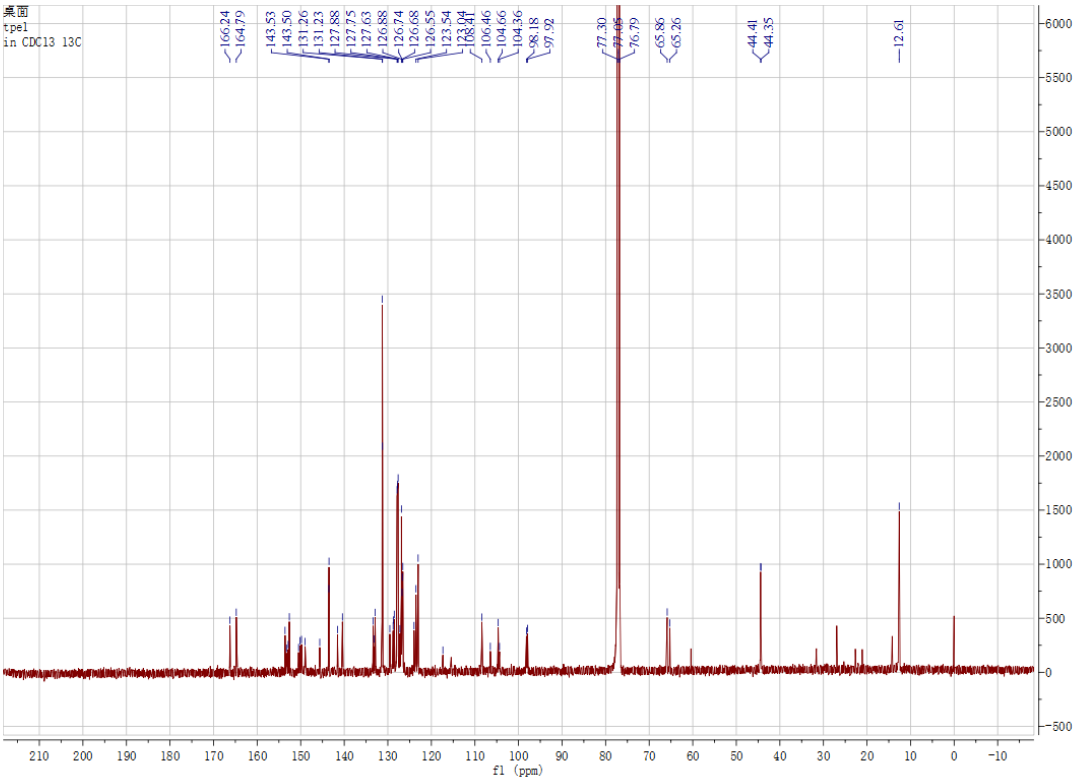

^{13}C NMR

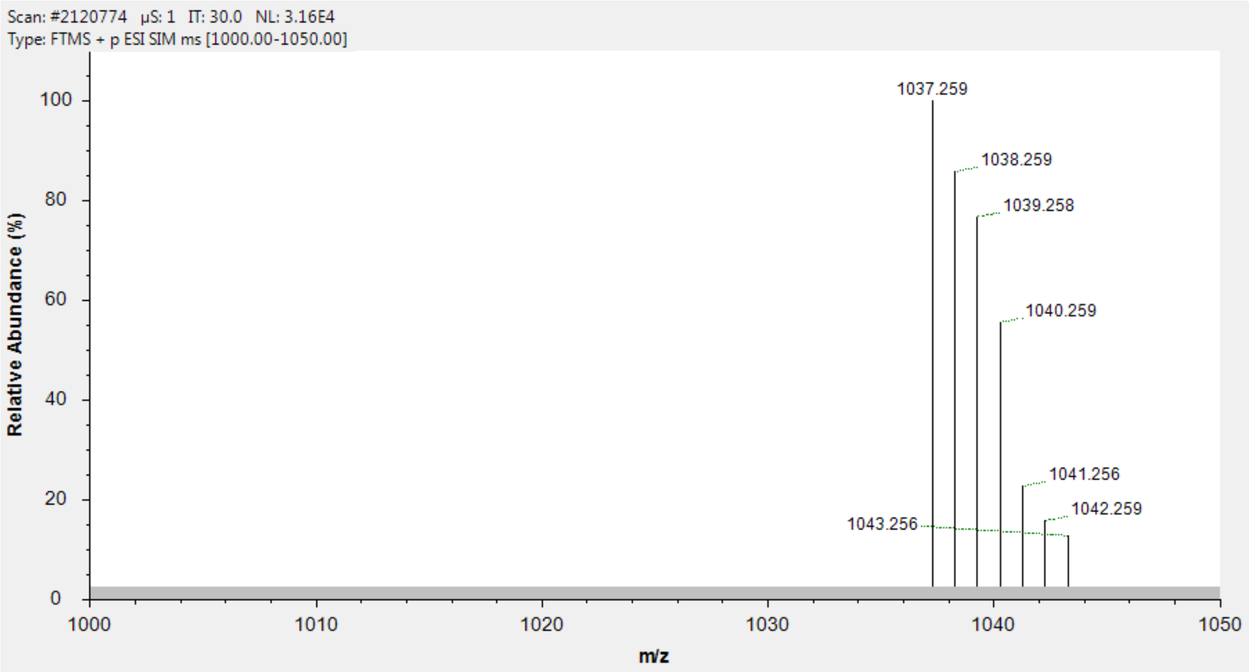

ESI-MS (M+3H^{+}: *m/z*=1037.259).

6. The characterization of A-T2.

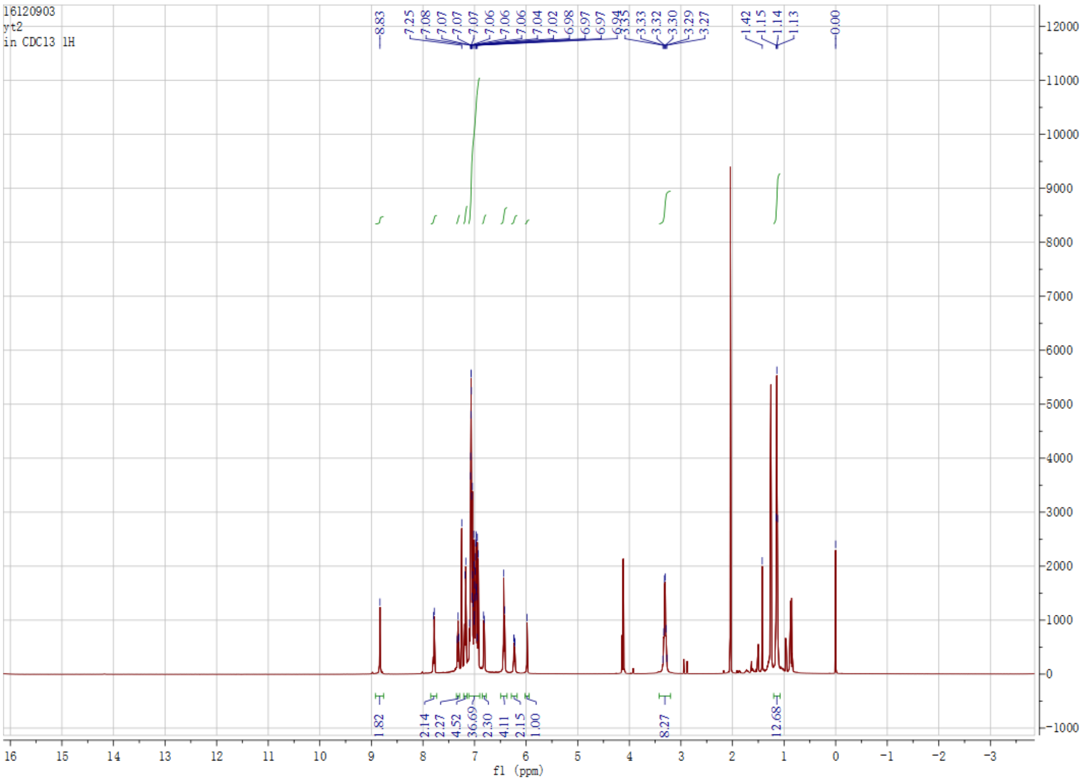

^{1}H NMR

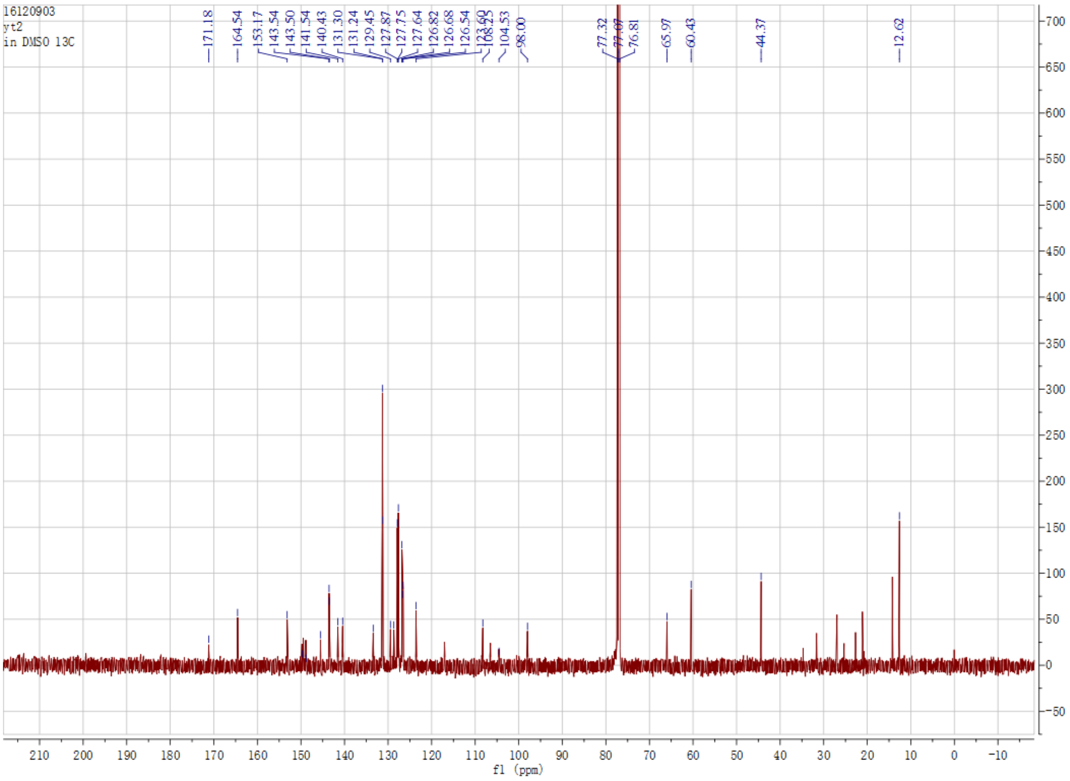

^{13}C NMR

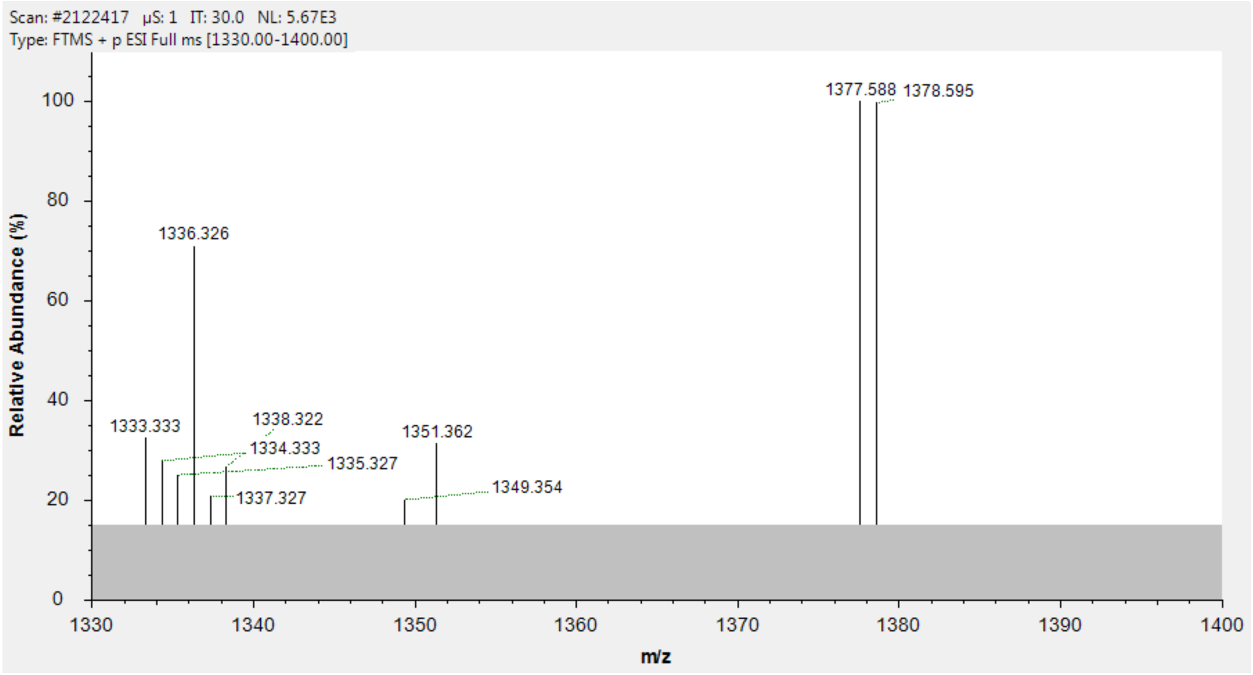

ESI-MS (M+H$^+$: *m/z*=1378.595)

7. The ESI-MS spectrum of A-T1-M^{n+}.

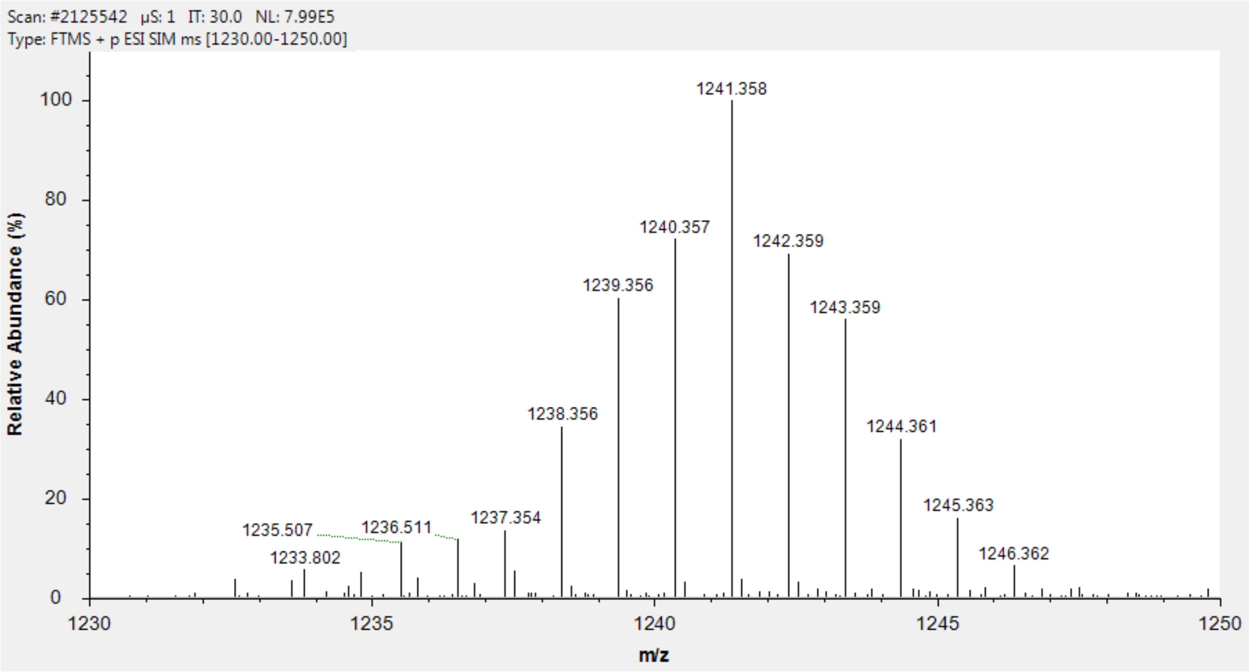

A-T1-Hg^{2+} (M+3H^{+}: *m/z*=1241.358)

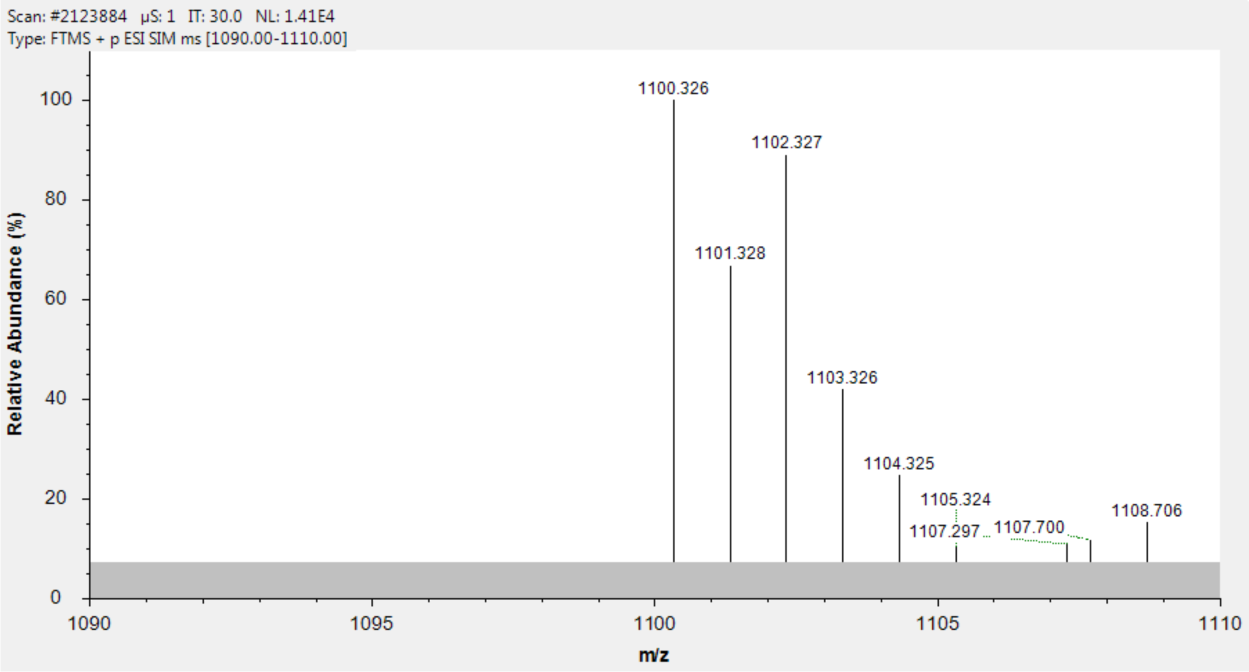

A-T1-Cu^{2+} (M+3H^{+}: *m/z*=1100.326)

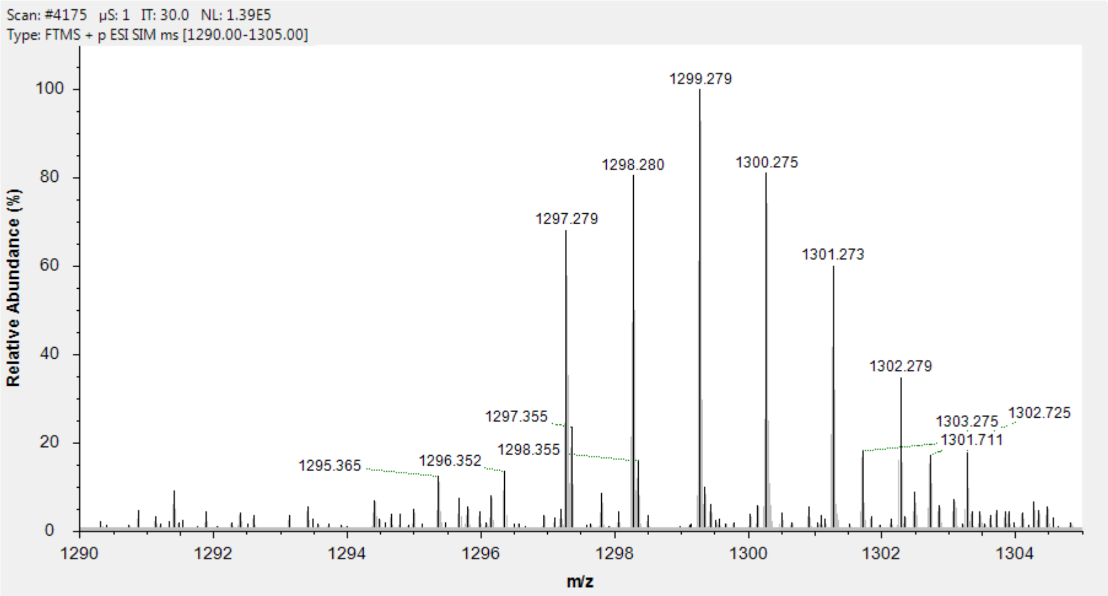

A-T1-Cu^{2+}-Hg^{2+} (M+H^{+}: *m/z*=1300.275)

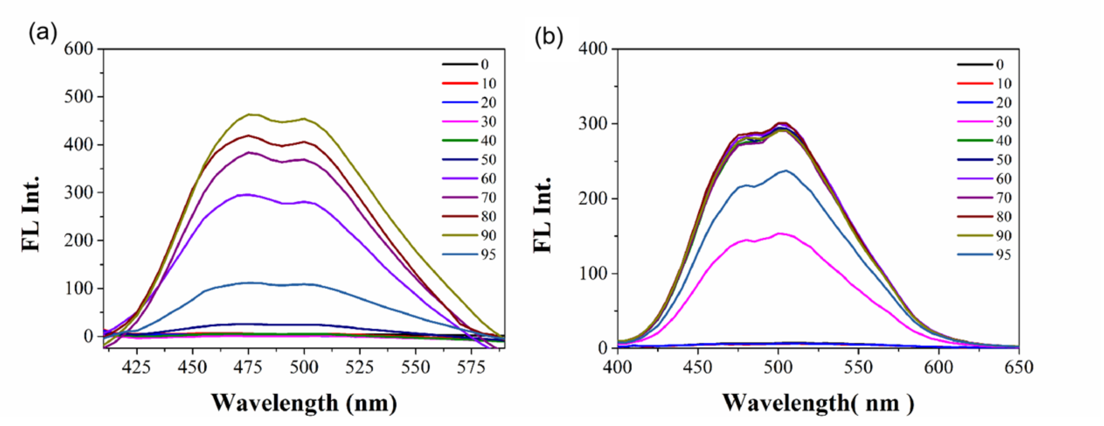

Fig. S1. The fluorescence spectra of AIE test of probe A-T1 (a) and A-T2 (b).

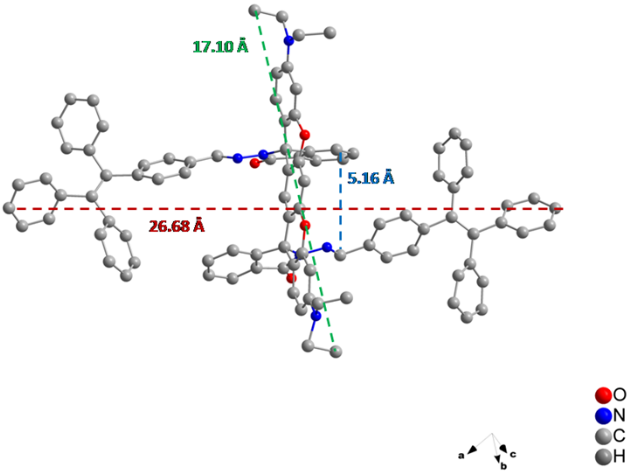

Fig. S2. The planar crystal structure of A-T2.

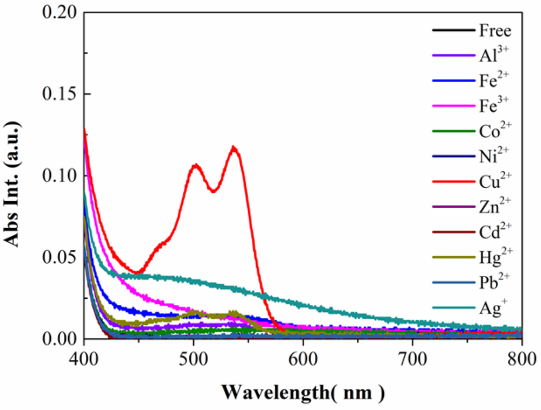

Fig. S3. Absorption spectra of absolute EtOH of A-T2 (10 μM) in the presence of various cations (10 equiv.).

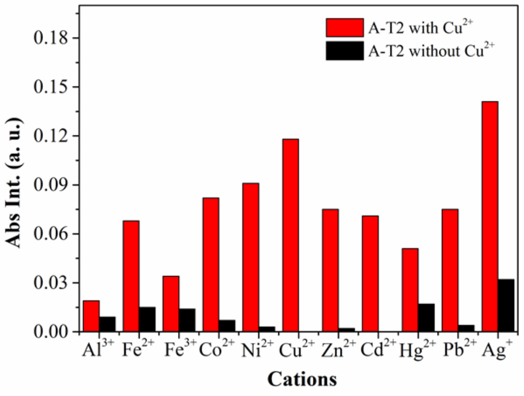

Fig. S4. The absorption spectra comparison of A-T2 with the addition of competitive cations (10 equiv, black bars) and Cu^{2+} (10 equiv, red bars) in EtOH.

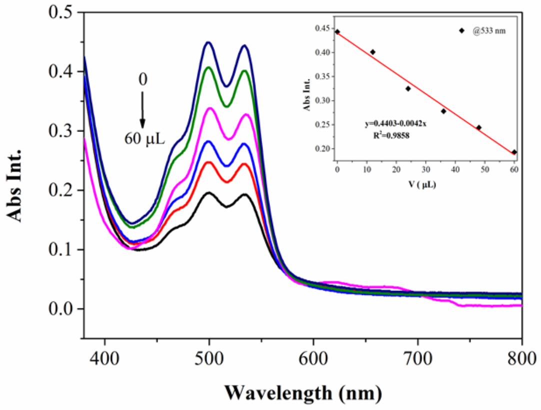

Fig. S5. Absorbance responses of the complexation between A-T1 and Hg^{2+} (10 μM) by adding S^{2-} in EtOH. The inset shows the absorbance intensity at 533 nm of the S^{2-}

volume.

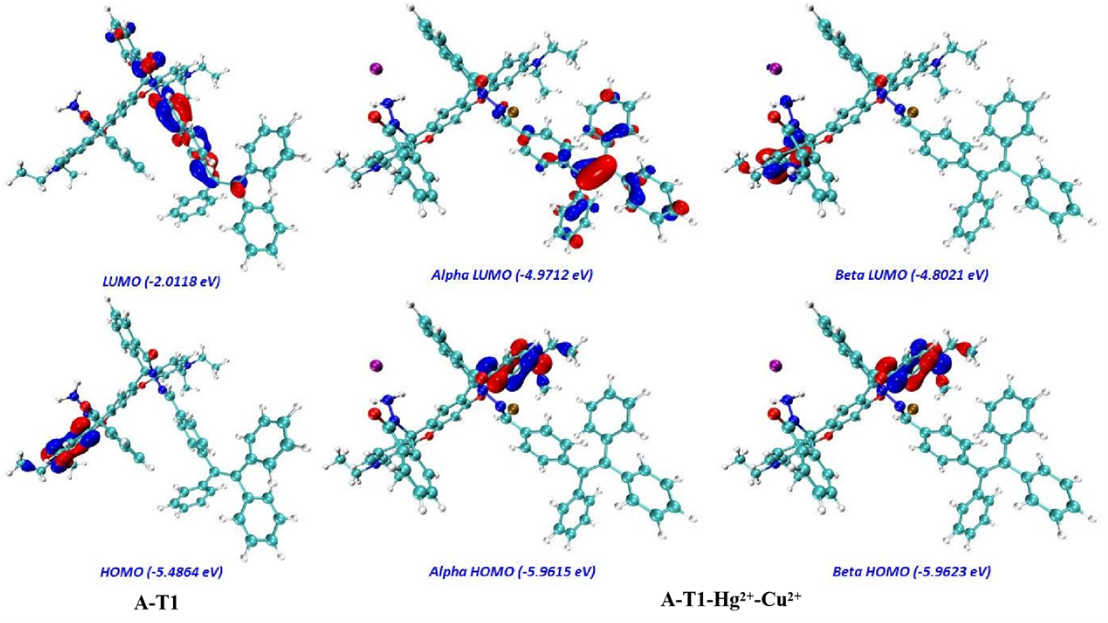

Fig. S6. The HOMO and LUMO between probe A-T1 and A-T1-Hg^{2+}-Cu^{2+}.

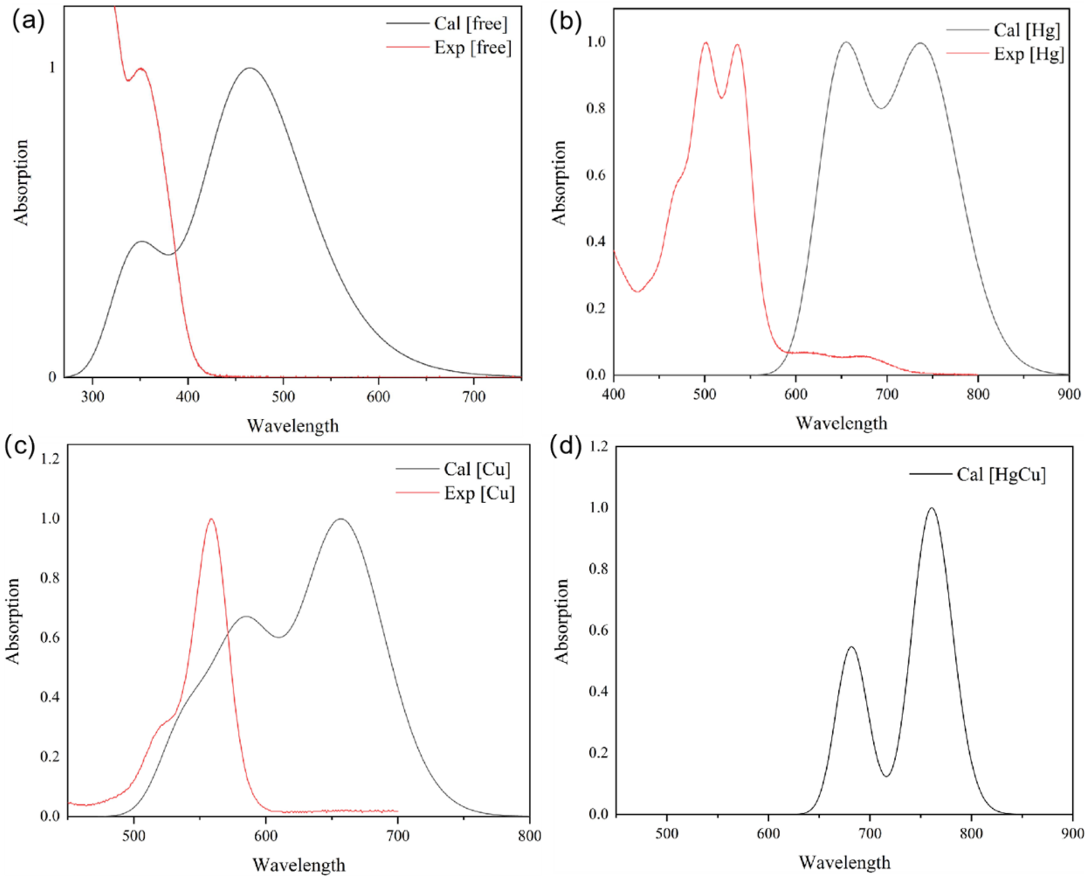

Fig. S7. The comparison of theoretical calculation and experimental spectral of (a) A-

T1, (b) A-T1-Hg^{2+}, (c) A-T1-Cu^{2+}, and (d) A-T1-Hg^{2+}-Cu^{2+}.

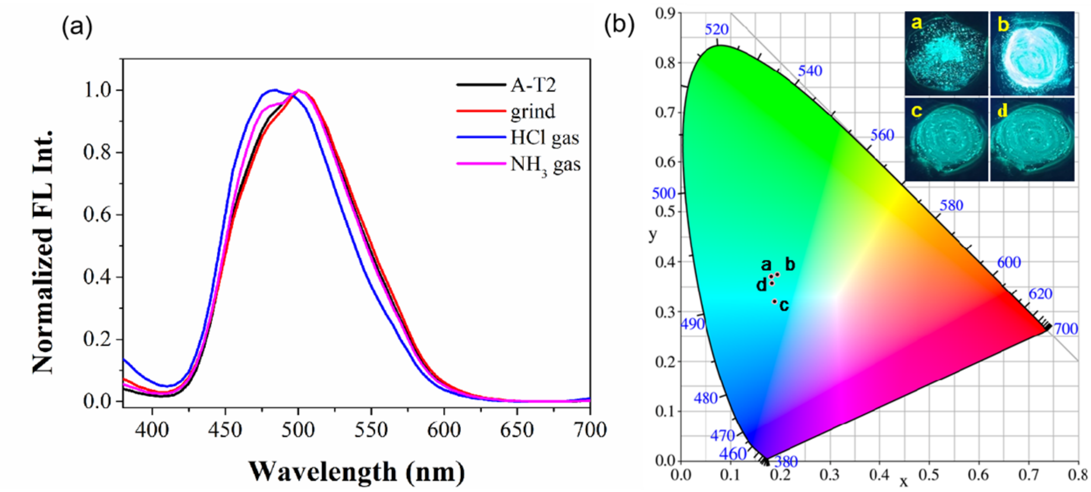

Fig. S8. a) Fluorescence comparison of A-T2 powder before and after treatment; b) CIE chromaticity diagram with coordinates corresponding to the surrounding environment of A-T2 powders (i) after grinding (ii) and exposure to HCl vapor (iii) and treated with NH_3 vapor again (iv).

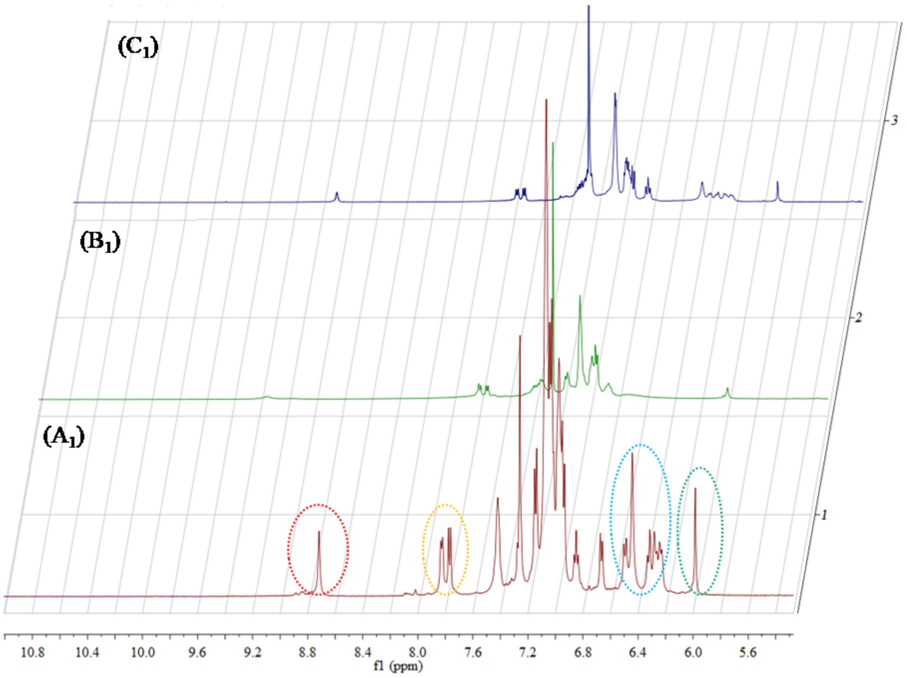

Fig. S9. The ^1H NMR spectrum of A-T1 (A_1), exposure to HCl vapor (B_1) and treated with NH_3 vapor again (C_1).

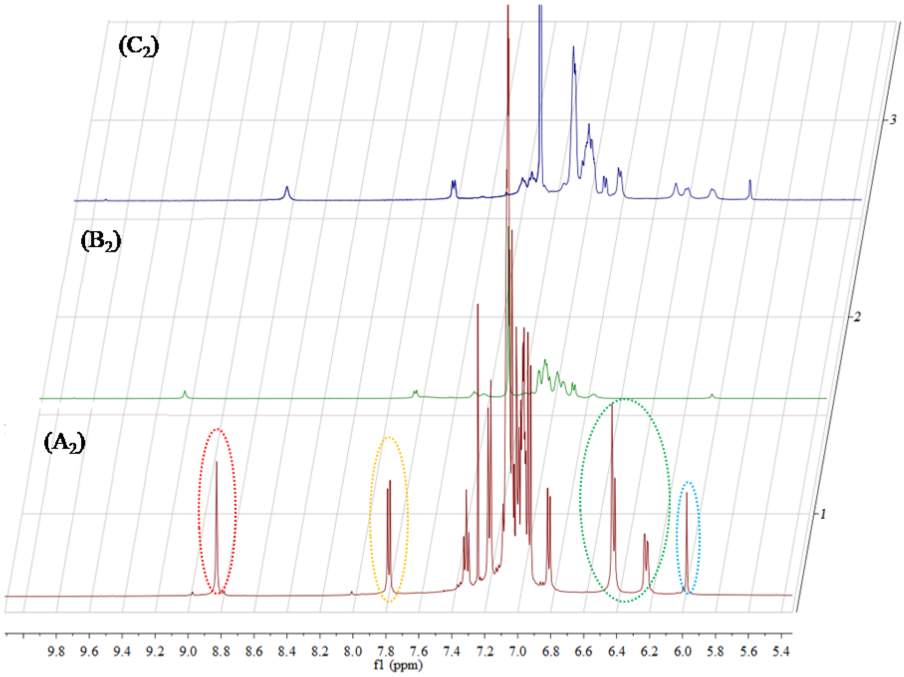

Fig. S10. The ^1H NMR spectrum of A-T2 (A_2), exposure to HCl vapor (B_2) and treated with NH_3 vapor again (C_2).

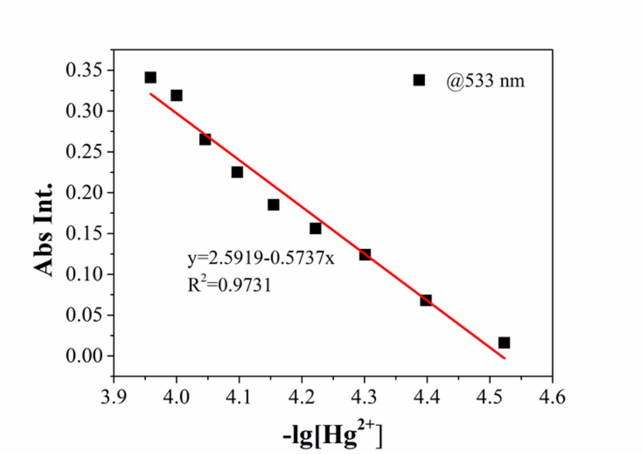

Fig. S11. The determination of detection limit for Hg^{2+} with probe A-T1 at 533 nm.

The detection limits (LOD = 3σ/slope) were calculated to be 12 μM.